Control of the Size of Cobalt Ferrite Magnetic Fluid

N. Moumen[†] and M. P. Pileni*,[†,‡]

Laboratoire SRSI, URA CNRS 1662, Universite P. et M. Curie, (Paris VI), BP 52, 4 Place Jussieu, 75231 Paris Cedex 05, France, and C.E.A.-C.E. Saclay, DRECAM-S.C.M, 91191 Gif sur Yuette Cedex, France

Received: August 21, 1995; In Final Form: September 29, 1995[⊗]

Cobalt and iron(II) dodecyl sulfate, $Co(DS)_2$ and $Fe(DS)_2$, are used to make nanosize magnetic particles. The size of the particles is controlled by the surfactant concentration. The average size of the particles, determined by transmission electron microscopy and from simulation of Langevin curves, varies from 2 to 5 nm, with 30−35% polydispersity in the size distribution. The magnetic studies are performed on particles having 2, 3, and 5 nm diameter, respectively. These particles are characterized by a superparamagnetic behavior. The saturation magnetization decreases with the particle size and is explained in terms of an increase in the noncollinear structure at the interface. For 5 nm particles, a cubic magnetocrystalline anisotropy is observed. On decreasing the size of the particles, the surface anisotropy strongly increases.

I. Introduction

Synthesis of nanoparticles, characterized by a low size distribution, is a new challenge in solid state chemistry. Due to their small size, the nanoparticles exhibit novel material properties which largely differ from the bulk solid state.[1] Many reports[2] on quantum size effect on semiconductor[3−4] or the emergence of metallic properties with the particle size[5−7] have been published during the past few years. A better understanding of magnetism is crucial not only for basic physics but also because of the great technological importance of ferromagnets in information storage,[8] color imaging,[9] bioprocessing,[10] and ferrofluids.[11] Ferromagnetism occurs even for clusters with less than about 30 atoms. As the size increases up to 700 atoms, the magnetic moments approach the bulk limit.[12]

Many investigations have been performed on particle having a size in the range of 10−30 nm. A superparamagnetic behavior[13−14] has been found. Small magnetic particles have surface properties that differ from those at the interior. The elucidation of these differences, however, is particularly difficult. The surface morphology, depending on the preparation technique, may vary. Passivation[15] and other requirements may introduce more than one phase. The interface and the surface,[16] whether vacuum, gas, or a coating,[17] may change the intrinsic surface properties. Interparticle interactions,[18] especially magnetic ones, may be important. The coating at the surface may change the intrinsic surface properties.[13,14]

Magnetic particles, Fe_3O_4, have been obtained on bilayer lipid membrane. Magnetic domains made of small particles have been obtained.[19]

Relatively little work exists on magnetic materials having sizes smaller than 10 nm. Nanocrystallites of γ-Fe_2O_3 having an average size of 8 nm have been synthesized by using a polymer matrix.[20] Recently, reverse micelles have been used to synthesize metallic or boride cobalt nanoparticles having an average size equal to 3 and 4 nm.[21−23]

In the present paper, oil in water micelles are used to make cobalt ferrite, $CoFe_2O_4$, magnetic fluid. The size of $CoFe_2O_4$ varies from 2 to 5 nm. The relative concentration of the reactants controls the size of the particles. The magnetic properties of particles differing by their size are presented.

II. Experimental Section

Sodium dodecyl sulfate, NaDS, was bought from BDH while iron chloride $Fe(Cl)_2$ and cobalt acetate, $Co(CH_3CO_2)_2$, were procured from Fluka. All the compounds have been sold as 99.99% purity.

The surface tension measurements of cobalt dodecyl sulfate, $Co(DS)_2$, and iron dodecyl sulfate, $Fe(DS)_2$, were performed on a Kruss equipment.

Conductivity measurements were performed by using a platinum electrode and a Tacussel CD 810 instrument.

A Philips transmission electron microscope (Model CM 20, 200 kV) was used to obtain electron micrographs of cobalt ferrite particles.

Magnetic studies were performed by using an S.Q.U.I.D. magnetometer. To prevent agglomeration, magnetic particles are dispersed in 50% of ethylene glycol in water. The volume fraction of magnetic particles is kept constant and equal to 1%.

III. Size Determination by TEM

A drop of the magnetic fluid is placed on a carbon film supported by a copper grid, and the solvent is evaporated. Histograms are obtained by measuring the diameter D_i of all the particles from different parts of the grid for an average number of particles close to 500. The standard deviation, σ, is calculated from the following equation:

$$\sigma = \{\sum[n_i(D_i - D)^2]/[N - 1]\}^{1/2}$$

where D and N are the average diameter and the number of particles, respectively.

IV. Treatment of Magnetic Data

The first magnetization curve of each sample is simulated from the Langevin relationship[24]

$$M(D) = M_s\{\mathrm{ctnh}(\mu H/kT) - (kT/\mu H)\}$$

with $\mu(D) = M_s\pi D^3/6$. M_s and M_s are the total saturation of the overall particles and of the bulk phase, respectively. In a

* Address correspondence to this author.
† Universite D. et M. Curie
‡ DRECAM-S.C.M
⊗ Abstract published in *Advance ACS Abstracts,* December 1, 1995.

0022-3654/96/20100-1867$12.00/0

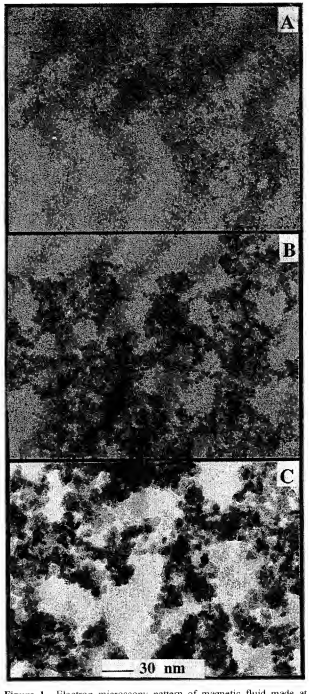

Figure 1. Electron microscopy pattern of magnetic fluid made at various surfactant concentrations keeping $[Co(DS)_2]/[Fe(DS)_2] = 0.325$, $[Co(DS)_2]/[NH_2CH_3] = 1.3 \times 10^{-2}$. $[Fe(DS)_2] = 6.5 \times 10^{-3}$ M (A), $[Fe(DS)_2] = 1.3 \times 10^{-2}$ M (B), $[Fe(DS)_2] = 2.6 \times 10^{-2}$ M (C).

given field H, $M(D)$ is the magnetization of particles characterized by a diameter, D.

Assuming a log normal size distribution, the magnetization of particles at a given field, H, is[24]

$$M = \int M(D)\, P(D)\, \mathrm{d}D$$

where $P(D)$ is the number of particles characterized by a given size, D.

Small ferromagnetic and ferrimagnetic particles are characterized by a superparamagnetism regime.[25,26] Their relaxation

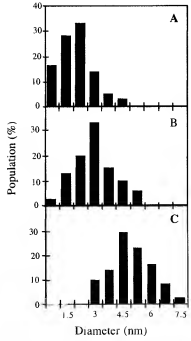

Figure 2. Histograms of magnetic fluid made at various surfactant concentrations keeping $[Co(DS)_2]/[Fe(DS)_2] = 0.325$, $[Co(DS)_2]/[NH_2CH_3] = 1.3 \times 10^{-2}$. $[Fe(DS)_2] = 6.5 \times 10^{-3}$ M (A), $[Fe(DS)_2] = 1.3 \times 10^{-2}$ M (B), $[Fe(DS)_2] = 2.6 \times 10^{-2}$ M (C).

times strongly decrease with decreasing the size of the particles. The magnetic moment follows the direction of the external field, and the coercive force appears to be negligible in contrast to permanent magnets. The first theory published by Neel[27] considers the relaxation as a random hopping of the magnetization vectors between the two easy directions in a particle.

The superparamagnetic relaxation time varies strongly with temperature. Most authors have assumed an exponential temperature dependence of the relaxation time, τ, as follows:[27]

$$\tau = \tau_0 \exp(K_A V/kT)$$

K_A, V, k, and T are the anisotropy energy constant, the volume of the particle, the Boltzmann's constant and temperature, respectively. The value of $\ln(\tau/\tau_0)$ can be deduced from the zero field cooled curve, ZFC, experimental time scale, $\tau = 1000$ s and $\tau_0 = 10^{-10}$ s[28]

$$\ln(\tau/\tau_0) \approx 30$$

The ZFC shows a peak corresponding to the blocking of particles at a typical volume V, determined by TEM. From the blocking temperature, T_B,[29] the anisotropy energy constant, K_A, of the particles can be calculated as follows:

$$K_A = 30(kT/V)$$

V. Synthesis of Cobalt and Iron Dodecyl Sulfate

Cobalt and iron dodecyl sulfate are made by mixing an aqueous solution of sodium dodecyl sulfate either with iron chloride or with cobalt acetate solution, as described in the literature.[30] An aqueous solution of 0.1 M of sodium dodecyl sulfate is mixed with 0.1 M of cobalt acetate. The solution is kept at 2 °C and a precipitate appears. It is washed several times with a 0.1 M cobalt acetate solution and recrystallized in distilled water. To make iron dodecyl sulfate, cobalt acetate is replaced by iron chloride and similar procedure as described

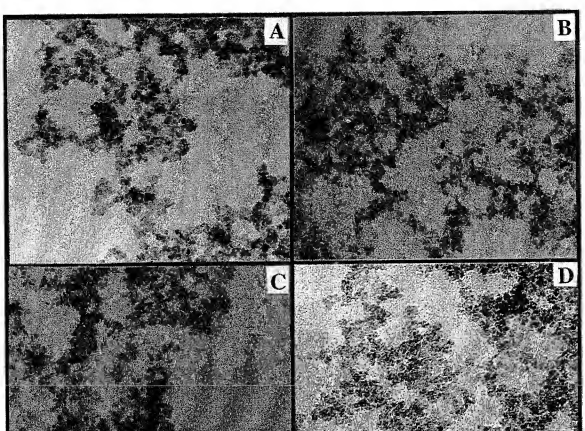

Figure 3. Electron microscopy patterns of magnetic fluid made at fixed reactants concentration, $[Co(DS)_2] = 0.42 \times 10^{-2}$ M, $[Fe(DS)_2] = 1.3 \times 10^{-2}$ M; $[NH_2CH_3] = 1$ M, and various sodium dodecyl sulfate concentrations [Na(DS)] = 0 M (A), [Na(DS)] = 1.56×10^{-2} M (B), [Na(DS)] = 6.56×10^{-2} M (C), [Na(DS)] = 1.65×10^{-1} M (D).

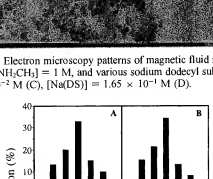

Figure 4. Histograms of magnetic fluid made at fixed reactants concentration, $[Co(DS)_2] = 0.42 \times 10^{-2}$ M, $[Fe(DS)_2] = 1.3 \times 10^{-2}$ M; $[NH_2CH_3] = 1$ M, and various sodium dodecyl sulfate concentration [Na(DS)] = 0 M (A), [Na(DS)] = 1.56×10^{-1} M (B), [Na(DS)] = 6.56×10^{-2} M (C), [Na(DS)] = 1.65×10^{-1} M (D).

for cobalt dodecyl sulfate is used. Cobalt dodecyl sulfate, $Co(DS)_2$, as well as iron dodecyl sulfate, $Fe(DS)_2$, form micellar aggregate at a critical micellar concentration, cmc. The cmc of $Co(DS)_2$ and $Fe(DS)_2$ has been determined from the break of the curve obtained by plotting either the variation of the surface tension or the conductivity versus the surfactant concentration. It is found equal to 1.34×10^{-3} and 1.40×10^{-3} M, respectively. On mixing $Co(DS)_2$ and $Fe(DS)_2$ at a given ratio $[Co(DS)_2]/[Fe(DS)_2] = 0.325$, the cmc of mixed micelles is quite unchanged compared to the one observed with the two surfactants separately (1.4×10^{-3} M). Cobalt ferrite particles in metal are composed of Fe(III) and Co(II). The syntheses have been performed in an excess of iron(II) because the oxidation yield of Fe(II) in Fe(III) is close to 65%.

VI. Results

1. Synthesis of $CoFe_2O_4$ Nanosized Particles. The procedure used is similar to that described in literature.[24] Methylamine, CH_3NH_3OH, is added to a mixed micellar solution formed by $Co(DS)_2$ and $Fe(DS)_2$ surfactants. The solution is stirred during 2 h with the appearance of a magnetic precipitate. The supernatant is removed and replaced by pure bulk aqueous phase. The precipitate is redispersed and a brown magnetic suspension is obtained. It is usually called magnetic fluid. The percentage of surfactant remaining in solution is less than 0.1 wt %.

Several syntheses have been performed by increasing the iron dodecyl sulfate concentration, from 6.5×10^{-3} to 2.6×10^{-2} M, keeping the $[Co(DS)_2]/[Fe(DS)_2]$ and $[Fe(DS)_2]/[CH_3NH_3OH]$ ratios equal to 0.325 and 1.3×10^{-2}, respectively. A drop

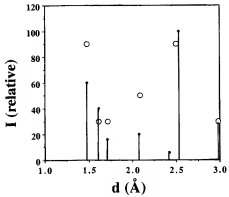

Figure 5. Electron diffractogram of 5 nm cobalt ferrite particles. The lines are given by standard reference tables and the points are the experimental data.

TABLE 1: Variation of the Particle Size and Polydispersity Determined by TEM

$[NaDS] \times 10^3$ (M)	0	0	0	1.56	6.56	16.5
$[Co(DS)_2] \times 10^3$ (M)	8.4	4.2	2.1	4.2	4.2	4.2
$[Fe(DS)_2] \times 10^2$ (M)	2.6	1.3	0.65	1.3	1.3	1.3
$[CH_3NH_2OH]$ (M)	2	1	0.5	1	1	1
D_{TEM} (nm)	5	3	2	2.8	2.6	2.4
σ (%)	23	30	37	28	31	32

of each magnetic fluid is placed on a carbon film supported by a copper grid. Figure 1 shows the electron micrograph of particles made at various $Fe(DS)_2$ concentrations. An increase in the particle size with $Fe(DS)_2$ concentration (Figure 2) is observed.

Similarly, the control of the particle size is obtained by increasing sodium dodecyl sulfate concentration and by keeping constant $Co(DS)_2$, $Fe(DS)_2$, and CH_3NH_2OH concentrations to 4.2×10^{-3}, 1.3×10^{-2}, and 1 M, respectively. Figures 3 and 4 show electron microscopy pattern and histograms of magnetic fluids obtained at various NaDS concentrations. A decrease in the particle size with increasing NaDS concentration (Table 1) can be observed.

2. Characterization of $CoFe_2O_4$ Nanosized Particles. Electron diffractogram patterns show a good agreement with the intense peaks listed for cobalt ferrite in standard reference tables (Figure 5). This indicates that the particles formed by using a micellar solution have the invert spinel crystalline structure as in the bulk phase. These results are confirmed by X-ray diffraction spectra. Electron microanalysis confirms the relative ratio of cobalt and iron elements in the cobalt ferrite particles (the percentages of the iron and cobalt elements are found equal to 65.63 and 34.37%, respectively).

3. Magnetic Properties. For particles having 5 nm as an average diameter the variation of magnetization, M (emu g^{-1}), with applied field, H(kOe), is given, at 300 K, in Figure 6. As expected, no hysteresis is observed, indicating that the particles are in a superparamagnetic regime. The saturation magnetization is found equal to 35 emu g^{-1} whereas for bulk phase it is equal to 78 emu g^{-1}.[31]

Figure 7 shows the magnetization curve, obtained at 200 K, for particles having an average diameter equal to 2, 3, and 5 nm, respectively. The initial susceptibility shows no hysteresis that is both the remanence and coercitivity are zero. This indicates a superparamagnetic behavior as expected for nanoscale dimension of the particles.

Table 2 shows an increase of the initial susceptibility with the particle size. The magnetic size of the particle can be deduced from simulation of Langevin relationship assuming a log normal size distribution[24] (Figure 6). A good agreement

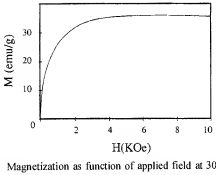

Figure 6. Magnetization as function of applied field at 300 K for 5 nm diameter.

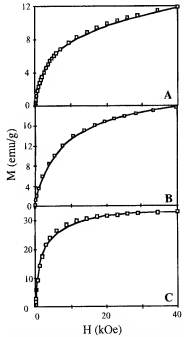

Figure 7. Magnetization as a function of applied field at 200 K for particles shown in Figure 1: (—) experimental data; (□) simulation of Langevin law.

TABLE 2: Variation of the Saturation Magnetization at 200 K (M_{s200} and 10 K (M_{s10}), the Average Diameter of the Particles Deduced from TEM D_{TEM}, and from Simulation, D_M, the Polydispersity in Size Determined by TEM, σ_{TEM}, and from simulation, σ_M, the Ratio of the Remanence and Saturation Magnetization at 10 K, M_{r10}/M_{s1}[0], the Coercitivity at 10 K, H_c, the Susceptibility at 200 K, χ_{200}, and the Anisotropy Constant, K_A

D_{TEM} (nm)	2	3	5
σ_{TEM} (%)	37	36	23
D_M (nm)	2	3	4.2
σ_M (%)	42	40	35
M_{s200} (emu/g)	14	22	35
M_{s10} (emu/g)	23	31	50
M_{s200}/M_{s10}	0.60	0.71	0.70
M_{r10}/M_{s10}	0.31	0.43	0.74
H_c (kOe)	5	7.5	9
$\chi_{200} \times 10^4$ (Oe)	2	2.4	4
$K_A \times 10^{-7}$ (erg cm^{-3})	7	3	1

between the size determined by TEM and that from the magnetization curve is observed (Table 2). The magnetic field needed to reach the saturation magnetization depends on the size of the particles. For particles having an average size equal to 2 and 3 nm, the saturation is not reached even for a magnetic field equal to 40 kOe, whereas it is observed with 5 nm particles.

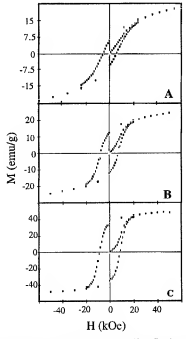

Figure 8. Magnetization as function of applied field at 10 K for 2 nm (A), 3 nm (B), and 5 nm (C) cobalt ferrite fluid. Volume fraction = 1%.

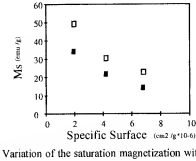

Figure 9. Variation of the saturation magnetization with the specific surface at 10 (□) and 200 K (■).

The saturation magnetization, deduced from zero extrapolation of M vs $1/H$, decreases with the decrease in the particle size (Table 2).

The magnetic particles are frozen in zero field at 10 K. Figure 8 shows the presence of hysteresis with an increase in the coercitivity with the particle size (Table 2). The ratio of the remanence to saturation magnetizations, M_r/M_s, deduced from the magnetization curve decreases with the decrease in particle size (Table 2).

Figure 9 shows a linear decrease in the saturation magnetization with the specific surface per area. The slope of the curve, is observed at 10 and 200 K, is found equal to 5.16×10^{-6} and 4.08×10^{-6} emu cm^{-2} at 10 and 200 K, respectively.

The samples are cooled in zero field to 10 K. Figure 10 shows the magnetization measured as a function of temperature in a 100 Oe field. As expected, the blocking temperature increases with the particle size (Table 2). From the blocking temperature, the anisotropy constant is deduced. Figure 11 shows a decrease in the anisotropy constant with the particle size. It is larger than the bulk value of cobalt ferrite material.

VII. Discussion

The mechanism of ferrite cobalt formation differs in homogeneous and micellar solutions. In homogeneous solution,[30] the magnetic fluid is obtained by solubilization of high iron (+3) and cobalt (+2) ions concentrations in aqueous solution ($[Co^{2+}] = 0.25$ M; $[Fe^{3+}] = 0.40$ M). After addition of methylamine the solution is stirred during 3 h at 380 K. In micellar solution, the concentration of reactants is smaller by several orders of magnitude (see above) and the experiment is performed at room temperature. Furthermore, in homogeneous solution the reaction starts with iron(+3) whereas it is iron (+2) in micellar solution.

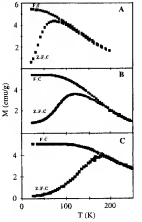

Figure 10. Zero field cooled (ZFC) and field cooled (FC) magnetization as function with temperature for a field of 100 Oe for 2 nm (A), 3 nm (B), and 5 nm (C) cobalt ferrite fluid. Volume fraction = 1%.

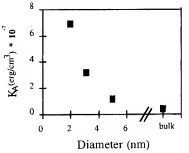

Figure 11. Variation of anisotropy energy, K_A, with the particle size.

The increase in the particle size, at fixed ratio of $[Co(DS)_2]/[Fe(DS)_2]$ and $[CH_3NH_3OH]/[Fe(DS)_2]$, with increasing $Fe(DS)_2$ concentration could be explained in term of changes of the structural micellar structure and of the oxidation degree of the reactants. As matter of fact, preliminary results,[32], from XANES and SAXS, in experimental conditions similar to those used to make the syntheses of the particles, indicate an increase in the oxidation degree of iron and cobalt ions and an increase in the micellar size with surfactant concentration. These changes would induce an increase in the number of nuclei which favors the formation of larger particles.

By keeping $Fe(DS)_2$, $Co(DS)_2$, and CH_3NH_3OH concentrations constant, the size of the cobalt ferrite decreases with an increase in sodium dodecyl sulfate concentration (Figure 3). The decrease in the size with increasing NaDS concentration could be attributed to several effects which act concomitantly. Addition of NaDS induces (i) a decrease in the average reactant per micelle; (ii) an increase in the aggregation number with formation of elongated micelles;[33] (iii) a decrease in the ionization degree of cobalt and iron ions.[34] All these parameters favor a decrease in the number of nuclei formed. The surfactant acts as a protecting agent and prevents against a growth of the particles. Similar behavior has been recently observed for copper metallic particles.[35]

At 300 K, for particles having 5 nm as an average diameter, the magnetization curve shows neither hysteresis nor remanence and coercitivity (Figure 5). This confirms the superparamagnetic behavior. The field needed to reach the saturation magnetization of bulk $CoFe_2O_4$ depends on the crystallographic direction. As matter of fact, for 100 and 111 atomic density orientations, the saturation magnetization is obtained for a field equal to 1 and 9 kOe, respectively.[36] At 300 K, for particles having an average diameter equal to 5 nm, the saturation magnetization is reached at 4 kOe. This value is in good agreement to the data obtained in bulk phase.

At 200 K, Figure 6 shows the superparamagnetic behavior for particles having 2, 3, and 5 nm diameter, respectively. The good agreement between the average size determined by TEM and from simulation of Langevin relationship (Table 2) indicates that the particle interactions can be neglected. This is confirmed by a progressive increase in the magnetic susceptibility with the average size of the particles.[37] This indicates that all the metallic atoms used to form the particles keep their magnetic particles properties. As has been previously observed for larger particles,[38–40] Table 2 shows a decrease in the saturation magnetization with the decrease in the particle size. Even for the larger particles (5 nm diameter), the saturation magnetization is less than the bulk value. This could be explained by an increase in noncollinearity structure when the particle size decreases. As matter of fact, it is well-known that in a spinel structure, the collinearity is a consequence of the fact that the magnetization of the A sublattice is antiparrallel to that of the B sublattice. Cobalt ferrite, known to have a relatively high magnetocrystalline anisotropy, has a noncollinear structure[13,40] which increases with coating by surfactant and with the decrease in the particle size in the range of few hundred angstroms. The decrease in the saturation magnetization with the particle size observed in the present paper cannot be attributed to formation of layers which remain nonmagnetic ("dead layers") as has been demonstrated for films made of ferromagnetic transition metals.[42–44] As matter of fact, Table 2 shows a good agreement between the size determined from TEM and deduced from Langevin curve. Furthermore, the thickness of such a layer is evaluated as 2 times the lattice parameter. This corresponds to 1.6 nm, for cobalt ferrite. This is not compatible with the magnetic properties observed for 2 nm particles.

Mollar et al.[44] have established, for $CoFe_2O_4$ particles having diameters ranging from 6.2 to 33 nm, that the saturation magnetization (measured at 4.2 K) in a high magnetic field decreases linearly with increasing the specific surface area. In the range of 2−5 nm, the measurements performed at 200 and 10 K show similar behavior as has been proposed by Mollar et al.[44] (Figure 8). The experiments performed by these two groups were not carried out at the same temperature (4.2 and 10 K, respectively) but the change of the saturation magnetization with temperature is small enough (Figure 8) to allow comparison with the present data. For particles having similar size (6.2 and 5 nm), a relatively good agreement between the saturation magnetization given by Mollar et al. and that in the present paper is observed. However, from Mollar et al. experiments, the slope of the linear relationship of the saturation magnetization with the specific surface area is found equal to 3.3×10^{-5} emu cm^2 at 4.2 K whereas from Figure 9 it is found equal to 5.2×10^{-6} emu cm^2. These differences could be due to the preparation mode and/or to the fact that the investigations have been performed in various size ranges. As matter of fact, Mollar et al. studied a change in the magnetic properties from 6.2 to 33 nm whereas it is from 2 to 5 nm in the present study. The extrapolation of the Molar et al. plot indicates that the zero saturation magnetization is reached for particles having a diameter equal to 4 nm. In our experiments, the saturation magnetization of 4 nm particles is found equal to 40 emu g^{-1}. The decrease in the saturation magnetization has been explained by the formation of a "dead layers" with a thickness equal to 2 times the lattice parameter which corresponds for cobalt ferrite to 1.6 nm. From the extrapolated Mollar plot, the particles having a diameter equal to 4 nm lose their magnetization. This could be explained by "dead layers" formation. From the present results in which the saturation magnetization of 4 nm particles is found equal to 40 emu g^{-1}, the assumption of "dead layer" formation can be excluded. Hence the decrease in the saturation magnetization with the decrease in the size of the particles observed in Figures 7, 8, and 9 can be attributed to an increase in the noncollinearity of the structure. An addition effect could be due to the remaining surfactant (0.1 wt %) present in the ferrofluid after synthesis.

The reduced remanence, M_r/M_s, depends on the magnetocrystalline anisotropy constant, the median diameter and the standard deviation of the system.[45] For random distribution of easy magnetic axes of particles with cubic magnetocrystalline anisotropy, the reduced remanence is expected to be equal to 0.83 at 0 K. For particles having 5 nm as an average diameter, Table 2 shows a M_r/M_s ratio equal to 0.74 at 10 K. The large remanence and coercivity values and the remanence to saturation magnetization ratio indicate that 5 nm particles consist of randomly oriented equiaxial particles with cubic magnetocrystalline anisotropy.[46] The progressive decrease of M_r/M_s ratio with the decrease in the particle size given in Table 2 could be explained as a progressive change of magnetocrystalline anisotropy from cubic to axial structure. The source of anisotropy might differ in ultrafine particle and the bulk material. Similar behavior has been observed for γ-Fe_2O_3 particles 6 nm in diameter.[47]

The anisotropy constant, K_A, is the sum of several terms taking into account the magnetocrystalline anisotropy, the shape and the surface of the particles, and the interactions between particles.[25] As expected, Figure 10 shows an increase in the blocking temperature with increasing the particle size. The anisotropy constant, determined from zero field cooling curve, is shown in Figure 11. Whatever the size, the anisotropy constant is always much larger than that obtained for bulk material. The decrease in the anisotropy constant with the particle size could be attributed to an increase in the surface anisotropy. The comparison between the change of M_r/M_s and K_A with the particle size indicates that K_A increases much more drastically than M_r/M_s with decreasing the particle size. K_A contains anisotropy terms such as surface and shape anisotropies and interactions between particles. From transmission electron microscopy no change in the shape of the particles is observed. The good agreement between the particle size determined by TEM and from simulation of Langevin curve indicates that the interactions between particles are negligible. Therefore, it is reasonable to conclude that the strong increase in the anisotropy with the decrease in size is due to surface anisotropy.

VIII. Conclusion

For the first time, the preparation of cobalt ferrite fluid having a size varying from 2 to 5 nm is described. This has been achieved by using functionalized surfactants. The size of the cobalt ferrite particles decreases when the total reactant concentration decreases and when the sodium dodecyl sulfate concentration increases. It is now possible to make various sizes of cobalt ferrite particles with 30% polydispersity in size distribution. These particles are characterized by a superpara-

magnetic behavior. The decrease in the saturation magnetization with the particle size is explained in term of an increase in the noncollinear structure at the interface. For 5 nm particles a cubic magnetocrystalline anisotropy is observed. By decreasing the size of the particles the surface anisotropy strongly increases.

Acknowledgment. The authors thank Dr. B. Barbara, Dr. S. Charles, and Dr. P. Veillet for fruitful discussions.

References and Notes

(1) For review see: Ozin, G. A. *Adv. Mater.* **1992**, *4*, 612.
(2) Pileni, M. P. *J. Phys. Chem.* **1993**, *97*, 6961.
(3) Pileni, M. P., Motte, L., Petit, C. *Chem. Mater.* **1992**, *4*, 338.
(4) Bawendi, M. G.; Steigerwald, M. L.; Brus, L. E. *Annu. Rev. Phys. Chem.* **1990**, *41*, 477 and reference therein.
(5) Petit, C.; Lixon, M. P.; Pileni, M. P. *J. Phys. Chem.* **1993**, *97*, 12974.
(6) Lisiecki, I.; Pileni, M. P. *J. Am. Chem. Soc.* **1993**, *115*, 3887.
(7) Lisiecki, I.; Pileni, M. P. *J. Phys. Chem.* **1995**, *99*, 5077.
(8) Gunther, L. *Phys. World* **1990**, *3*, 28.
(9) Ziolo, R. F. U.S. Patent **1984**, *4*, 474.
(10) McMichael, R. D.; Shull, R. D.; Swartzendruber, L. J.; Bennett, L. H.; Watson, R. E. *J. Magn. Magn. Mater.* **1992**, *111*, 29.
(11) Anton, I., et al. *J. Magn. Magn. Mater.* **1990**, *85*, 219.
(12) Billas, M. L. I., Châtelain, A., de Heer W. A. *Science* **1994**, *265*, 1682.
(13) Haneda, K. *Can. J. Phys.* **1987**, *65*, 1233.
(14) Norrish, A. H. In *Studies of Magnetic Properties of Fine Particles and Their Relevance to Materials Science*; Dormann, J. L., Fiorani, D., Eds.; Elsevier Science Publishers: New York, 1992, p 181.
(15) Gangopadhyay, S.; Hadjipanayis, G. C.; Sorensen, C. M.; Klabunde, K. J. *IEEE Trans. Mag.* **1993**, *29*, 2619.
(16) Shinjo, T. *J. Phys.* **1979**, *J*, 6.
(17) Berkowitz, A. E.; Lahut, J. A.; Jacobs, I. S.; Levinson, M.; Forester, D. W. *Phys. Rev. Lett.* **1975**, *34*, 594.
(18) Fere, R.; Barbara, B.; Fruchart, D.; Wolfers, P. *J. Magn. Magn. Mater.* **1995**, *140*, 385.
(19) Zhao, X. K.; Herve, P. J.; Fendler, J. H. *J. Phys. Chem.* **1989**, *93*, 908.
(20) Ziolo, R. F., Giannelis, E. P., Weinstein, B. A.; O'Horo, M. P.; Ganguly, B. N.; Mehrotra, V., Russell, M. W.; Huffman, D. R. *Science* **1992**, *257*, 219.
(21) Chen, J. P.; Lee, K. M.; Sorensen, C. M.; Klabunde, K. J.; Hadjipanayis, G. C. *J. Appl. Phys.* **1994**, *75*, 5876.
(22) Chen, J. P., Sorensen, C. M.; Klabunde, K. J.; Hadjipanayis, G. C. *J. Appl. Phys.* **1994**, *76*, 6316.
(23) Petit, C.; Pileni, M. P., submitted for publication.
(24) Charles, S. W.; Popplewell, J. In *Ferromagnetic Materials*, Wolhlfarth, Ed.; North Holland Publishing Co.: Amsterdam, 1982, Vol 2.
(25) Dormann, J. L. *Rev. Phys. Appl.* **1981**, *16*, 275.
(26) Bean, C. P.; Livingston, J. D. *J. Appl. Phys.* **1959**, *30*, 120S.
(27) Neel, L. *Ann. Goephys.* **1949**, *5*, 99.
(28) Vincent, E.; Hamman, J.; Prené, P., Tronc, E. *J. Phys. Fr.* **1994**, *4*, 273.
(29) The blocking temperature is defined as the temperature in which 50% of particles are in the superparamagnetic regime and 50% are ferromagnetic.
(30) Charles, S. W. *J. Magn. Magn. Mater.* **1987**, *65*, 350.
(31) *Ferromagnetic Materials*, Wohlfarth, E. P., Ed.; North Holland Publishing Co.: Amsterdam, 1982.
(32) Lisiecki, I.; Moumen, N.; Pileni, M. P.; private communication.
(33) Hayter, J.; Penfold, B *Colloid Polym. Sci.* **1983**, *261*, 1022.
(34) Moroi, Y., Motomura, K.; Matuura, R. *J. Colloid Interface Sci.* **1974**, *46*, 111.
(35) Lisiecki, I.; Billoudet, F., Pileni, M. P. *J. Phys. Chem.*, in press.
(36) *Landolt-Bornstein Numerical data and functional relationships in Science and Technology*; Hellwege, K. H., Hellwege, A. M., Eds.; Springer-Verlag: Berlin, 1980; Vol. 12.
(37) Chantrell, R. M. W.; Popplewell, J.; Charles, S. W. *IEEE Trans Magn. Mag.* **1972**, *5*, 975.
(38) Berkowitz, A. E., Schuele, W. J.; Flanders, P. J. *J. Appl. Phys.* **1968**, *39*, 1261.
(39) Haneda, K.; Morrish, A. H. *IEEE Trans. Mag.* **1989**, *25*, 2597.
(40) de Backer, P. M.; De Grave, E.; Vandenberghe, R. E.; Bowen, L. H., *Hyperfine Interact.* **1990**, *54*, 493.
(41) Berkowitz, A. E.; Lahut, J. A., Van Buren, C. E. *IEEE Trans. Mag.* **1980**, 184.
(42) Liebermann, L.; Fredkin, D. R., Shore, H. B. *Phys. Rev. Lett.* **1969**, *22*, 539.
(43) Liebermann, L., Clinton, J., Edwards, D. M., Mathon, J. *Phys. Rev. Lett.* **1970**, *25*, 232.
(44) Mollard, P.; Germi, P.; Rousset, A. *Physica B+C* **1977**, *86–88*, 1393.
(45) Charles, S. W.; Chandrasekhar, R.; O'Grady, K.; Walker, M. *J. Appl. Phys.* **1988**, *64*, 5840.
(46) *Magnetism and Metallurgy*; Berkowitz, A. E., Kneller, E., Eds., Academic Press: New York, 1969; Vol. 1, Chapter 8.
(47) Coey, J. M. D.; Khalafalla. *Phys. Status Solidi A*, **1972**, *11*, 229.

JP9524136